Published in final edited form as:
Sci Transl Med. 2011 November 9; 3(108): 108ra114. doi:10.1126/scitranslmed.3002950.

Differential inhibitor sensitivity of anaplastic lymphoma kinase variants found in neuroblastoma

Scott C. Bresler[1,2,3,8], **Andrew C. Wood**[4,8], **Elizabeth A. Haglund**[4], **Joshua Courtright**[4], **Lili T. Belcastro**[4], **Jefferson S. Plegaria**[4], **Kristina Cole**[4], **Yana Toporovskaya**[4], **Huaqing Zhao**[5], **Erica L. Carpenter**[4], **James G. Christensen**[6], **John M. Maris**[4,7], **Mark A. Lemmon**[1,2,9], and **Yaël P. Mossé**[4,9]

[1]Department of Biochemistry and Biophysics, Perelman School of Medicine at the University of Pennsylvania, Philadelphia, PA 19104-6059, USA.

[2]Graduate Group in Biochemistry and Molecular Biophysics, Perelman School of Medicine at the University of Pennsylvania, Philadelphia, PA 19104, USA.

[3]Medical Scientist Training Program, Perelman School of Medicine at the University of Pennsylvania, Philadelphia, PA 19104, USA.

[4]Division of Oncology and Center for Childhood Cancer Research, Children's Hospital of Philadelphia; Department of Pediatrics, Perelman School of Medicine at the University of Pennsylvania, PA 19104, USA.

[5]Biostatistics and Data Management Core, Children's Hospital of Philadelphia; Department of Pediatrics, University of Pennsylvania School of Medicine, Philadelphia, PA 19104, USA.

[6]Department of Cancer Research, Pfizer Global Research and Development, La Jolla Laboratories, La Jolla, CA 92121, USA.

[7]Abramson Family Cancer Research Institute, Perelman School of Medicine at the University of Pennsylvania, Philadelphia, PA 19104, USA.

Abstract

Activating mutations in the anaplastic lymphoma kinase (*ALK*) gene were recently discovered in neuroblastoma, a cancer of the developing autonomic nervous system that is the most commonly diagnosed malignancy in the first year of life. The most frequent *ALK* mutations in neuroblastoma cause amino acid substitutions (F1174L and R1275Q) in the intracellular tyrosine kinase domain of the intact ALK receptor. Identification of ALK as an oncogenic driver in neuroblastoma suggests that crizotinib (PF-02341066), a dual-specific inhibitor of the ALK and Met tyrosine kinases, will be useful in treating this malignancy. Here, we assessed the ability of crizotinib to inhibit proliferation of neuroblastoma cell lines and xenografts expressing mutated or wild-type

[9]Correspondence should be addressed to Y.P.M. or M.A.L. at: Yaël P. Mossé, Division of Oncology, Center for Childhood Cancer Research, Children's Hospital of Philadelphia, CTRB 3056, 3501 Civic Center Boulevard, Philadelphia, PA 19104, Tel: (215) 590-0965, Fax: (267) 426-0685, mosse@email.chop.edu, Mark A. Lemmon,Department of Biochemistry and Biophysics, Perelman School of Medicine at the University of Pennsylvania,809C Stellar-Chance Laboratories, 422 Curie Boulevard,Philadelphia, PA 19104-6059, Tel: (215) 898-3072, Tel: (215) 898-3072, mlemmon@mail.med.upenn.edu.
[8]These authors contributed equally to the work described in this manuscript

Author contributions: S.C.B. designed and performed *in vitro* studies of ALK-TKD, analyzed and interpreted data, and drafted the manuscript. A.C.W. designed and performed cellular and *in vivo* experiments, analyzed and interpreted data, and drafted the manuscript. E.A.H., J.C., L.T.B., J.S.P., K.C., Y.T., and H.Z. made important contributions to cellular and *in vivo* experiments and/or data analysis. E.L.C., J.G.C., J.M.M., Y.P.M., and M.A.L. guided study design, implementation and interpretation, provided conceptual direction, and wrote the manuscript with S.C.B. and A.C.W.

Competing interests: J.G.C. is an employee of Pfizer, the developer of crizotinib. Other authors declare that they have no competing interests.

ALK. Crizotinib inhibited proliferation of cell lines expressing R1275Q-mutated ALK and a cell line with amplified and overexpressed wild-type ALK. By contrast, cell lines harboring F1174L-mutated ALK were relatively resistant to crizotinib. Biochemical analyses revealed that this reduced susceptibility of F1174L-mutated ALK to crizotinib inhibition results from an increased ATP-binding affinity (as also seen in acquired resistance to EGFR inhibitors), and should be surmountable with higher doses of crizotinib and/or with higher affinity inhibitors.

INTRODUCTION

Neuroblastoma arises in the developing autonomic nervous system, and is the most commonly diagnosed malignancy in the first year of life. The disease shows a wide range of clinical phenotypes; tumors regress spontaneously in some patients, whereas most have aggressive metastatic disease (1). Neuroblastoma remains a leading cause of childhood cancer mortality despite dramatic escalations in dose-intensive chemoradiotherapy, and long-term survivors experience significant treatment-related morbidity (2).

One promising therapeutic target in neuroblastoma is the anaplastic lymphoma kinase (ALK), an orphan receptor tyrosine kinase (RTK) normally expressed only in the developing nervous system (3). Oncogenic ALK alterations were first described in anaplastic large cell lymphoma (4), where a chromosomal translocation leads to production of a fusion protein with the ALK intracellular region fused to an amino-terminal fragment of nucleophosmin (NPM). Other ALK fusion proteins are potent oncogenic drivers in a subset of non-small cell lung cancers (NSCLC) (5), and drive inflammatory myofibroblastic tumors (IMTs) as well as other cancers (6). In neuroblastoma, germline activating point mutations in the intact *ALK* gene were revealed by linkage analysis of a set of families with highly penetrant autosomal dominant disease (7). In addition, somatic *ALK* mutations were found in ~10% of sporadic neuroblastoma cases (7–11). The most frequently observed substitutions, together accounting for >80% of sporadic *ALK* mutations in neuroblastoma samples (12), were F1174L and R1275Q – which lie in key regulatory regions of the ALK receptor kinase domain. Mutations in the intact *ALK* gene have also recently been reported in anaplastic thyroid cancer (13).

ALK tyrosine kinase activity can be inhibited by crizotinib (PF-02341066), a small molecule ATP-competitive inhibitor that selectively targets both the ALK and Met RTKs (14). A recent phase I study of crizotinib demonstrated safety and tolerability in humans, as well as tumor shrinkage or stable disease in most patients with ALK-dependent NSCLC (15). Crizotinib is also in early phase clinical testing in patients with neuroblastoma. As with other tyrosine kinase inhibitor therapies, acquired resistance to crizotinib is already beginning to emerge (16–18). Understanding how mutations affect both kinase activity and inhibitor sensitivity is imperative for guiding future clinical use of ALK-targeted inhibitors. In this report, we explore the ability of crizotinib to inhibit intact ALK in neuroblastoma cell line models, and analyze the effects of the two most common activating mutations seen in neuroblastoma on ALK's tyrosine kinase activity. We find that the F1174L mutation – while activating – reduces ALK sensitivity to crizotinib in xenograft, cell-line and enzymatic assays, consistent with the recent surprising report of this mutation as an acquired resistance mutation in an oncogenic ALK fusion protein (17). Compared with the R1275Q activating mutation, we find that an F1174L substitution increases ATP binding affinity, leading to crizotinib resistance that should be surmountable with higher doses of crizotinib and/or new higher-affinity inhibitors.

RESULTS

The effect of crizotinib on growth of neuroblastoma-derived cell lines depends on *ALK* genomic status and the specific mutation

To assess how the most common ALK mutations in neuroblastoma (F1174L and R1275Q) affect intrinsic ALK activity, we expressed full-length ALK variants in human retinal-pigmented epithelial (RPE) cells immortalized with telomerase reverse transcriptase (hTERT-RPE1). We selected RPE cells because they are derived from human neural crest like neuroblastomas, but express no endogenous ALK (Fig. 1A). Whereas wild-type ALK expressed in hTERT-RPE1 cells is not detectably phosphorylated (Fig. 1A), both R1275Q and F1174L-mutated ALK show robust autophosphorylation in immunoblots using an ALK pY1604-specific antibody, regardless of the presence of serum in the medium (Fig. 1A, middle panels). Thus, both common neuroblastoma mutations cause constitutive ALK activation to similar extents, as seen in Ba/F3 (10), NIH3T3 (9, 19) and PC12 cells (20), as well as numerous neuroblastoma-derived cell lines (7, 10, 11, 19). Consistent with previous reports (19, 21), two ALK species are always observed. Full-length ALK migrates as a 220kDa protein, and the 140kDa species is a cleavage product lacking part of the extracellular region (21).

We and others have shown that RNAi knockdown of ALK, or pharmacological inhibition of ALK kinase activity, has an anti-proliferative effect in several *ALK*-mutated neuroblastoma cell lines (7, 9–11), associated with G1 arrest and increased apoptosis (10). To exploit this observation clinically, we assessed cytotoxicity of the ALK/Met inhibitor crizotinib (PF-02341066) in cell models for neuroblastoma. We first analyzed the ability of crizotinib to inhibit substrate-adherent growth of a panel of eighteen human neuroblastoma-derived cell lines. The 18 cell lines were chosen to represent *ALK* genomic status in primary tumors, and have all previously been well characterized. Analysis of concentration-response curves across a 4-log crizotinib dose range (1 – 10,000nM) revealed significant differences in IC_{50} that correlated with *ALK* status. As illustrated in Fig. 1B, cell lines harboring an *ALK* aberration (amplification or mutation) were significantly more sensitive to growth inhibition by crizotinib than cell lines with wild-type *ALK* status ($p = 0.001$, two sided exact Wilcoxon-Mann-Whitney test). To ensure that crizotinib cytotoxicity in this assay reflects ALK inhibition, we confirmed that the drug reduces phospho-ALK levels (see below). In addition, since crizotinib also inhibits Met kinase activity (14), it was important to exclude Met inhibition as a mechanism. We confirmed that none of the crizotinib-inhibited neuroblastoma cell lines displays significant phospho-Met levels (fig. S1). Moreover, RNAi knockdown of Met in a panel of cell lines with altered *ALK* genomic status had no growth inhibitory effect (table S1). The enhanced crizotinib sensitivity of almost all neuroblastoma cell lines harboring *ALK* mutation or amplification (Fig. 1B) strengthens the argument for ALK inhibition as a useful therapeutic strategy in neuroblastoma.

Mutation-specific stratification of crizotinib sensitivity in neuroblastoma cell lines (Fig. 1B) may have significant implications for clinical use of this drug. Cell lines expressing F1174L-mutated ALK were marginally significantly less sensitive to growth inhibition by crizotinib than those expressing R1275Q-mutated ALK ($p = 0.067$; two sided exact Wilcoxon-Mann-Whitney test), justifying further investigation. This result was initially quite unexpected, since the F1174L and R1275Q mutations appear to promote similar degrees of constitutive ALK activation (Fig. 1A), and siRNA knockdown of either variant inhibits growth of the relevant cell lines (7). Assuming a similar oncogenic driver role for both ALK variants, the data in Fig. 1B suggest that the F1174L mutation may also promote crizotinib resistance. Indeed, an F1174L mutation was recently found to cause acquired crizotinib resistance in a patient with an inflammatory myofibroblastic tumor (IMT) driven by constitutively active RANBP2-fused ALK (17). The F1174L substitution may therefore combine the

characteristics of an activating mutation and a resistance mutation, understanding of which is crucial for developing ALK-targeted therapy.

Tumor growth driven by F1174L-mutated ALK also shows reduced sensitivity to crizotinib *in vivo*

We next asked whether the two ALK variants show differential crizotinib sensitivity *in vivo*, employing xenograft models of neuroblastoma. We tested a pharmacologically relevant crizotinib dose (100mg/kg/day for 4 weeks) against serially passaged human neuroblastoma cells xenografted in the flank of CB17 immunodeficient mice (14). As shown in Fig. 2A, crizotinib caused tumor regression within three weeks in all NB1643 xenografts (R1275Q-ALK), and complete regression was sustained over the fourth week of dosing ($p < 0.0001$). Assessment of phospho-ALK levels by immunoblotting NB1643 xenograft lysates harvested after 48 hours of crizotinib administration (4 hours after final dose) confirmed inhibition of ALK phosphorylation (Fig. 2A inset). Consistent with the differential sensitivity suggested *in vitro*, xenografts harboring F1174L-ALK (SH-SY5Y and NBSD) were substantially less responsive to crizotinib. No tumor regression was observed in crizotinib-treated SH-SY5Y xenografts (Fig. 2B), although tumor growth was significantly delayed ($p < 0.0001$) and the time taken to reach the study endpoint (tumor volume ≥ 1.5 cm^3) was extended by an average of 7.7 days ($p < 0.0001$). Crizotinib also failed to reduce tumor volume ($p = 0.29$) in NBSD (F1174L) xenografts (Fig. 2C), although the time to reach the study endpoint was again extended by a mean 3.7 days ($p = 0.04$). These results argue that tumors driven by F1174L-mutated ALK are significantly less sensitive to crizotinib *in vivo*. Crizotinib treatment led to complete tumor regression in NB1 xenografts with amplified, overexpressed wild-type ALK (Fig. 2D), but not in NB-EBc1 or SKNAS xenografts that have no amplification (Fig. 2E,F). Crizotinib treatment delayed tumor growth ($p < 0.0001$) in NB-EBc1 xenografts (low phospho-ALK levels, but no mutation or amplification), but had no detectable effect ($p = 0.70$) in SKNAS xenografts, which express low levels of wild-type ALK and show no detectable phospho-ALK (Fig. 2F).

The F1174L mutation reduces crizotinib-sensitivity of ALK autophosphorylation

The reduced crizotinib sensitivity of cell lines and xenografts harboring F1174L-mutated ALK prompted us to analyze the effects of this drug on constitutive ALK activity in representative cell lines: NB1643 cells (which express R1275Q ALK), and SH-SY5Y cells (which express F1174L ALK). Crizotinib treatment abrogated Y1604 phosphorylation of ALK in both cell lines, but at different doses (Fig. 3). In NB1643 (R1275Q) cells, ALK phosphorylation was essentially abolished at 100nM crizotinib (IC_{50} ~ 10nM), whereas complete inhibition of F1174L ALK phosphorylation in SH-SY5Y cells required almost 1μM crizotinib (IC_{50} ~ 50nM). Akt phosphorylation followed similar trends (fig. S2), consistent with a previous report that ALK inhibition promotes apoptosis in neuroblastoma cell lines (10). Crizotinib resistance of cells harboring the ALK F1174L mutation therefore appears to arise from less potent inhibition of constitutive ALK activity and thus of downstream survival signaling.

F1174L and R1275Q mutations promote autophosphorylation of the ALK kinase domain

To understand why F1174L- and R1275Q-mutated ALK have different crizotinib sensitivities, and how the mutations enhance kinase activity, we turned to *in vitro* studies of the ALK tyrosine kinase domain (ALK-TKD), purified from baculovirus-infected Sf9 cells as a histidine-tagged protein. To generate fully dephosphorylated (inactive) ALK-TKD, YopH phosphatase treatment was used to reverse spontaneous autophosphorylation arising during production (Supplementary Methods). For comparative studies, fully autophosphorylated ALK-TKD was generated by clustering the protein on lipid vesicles bearing NTA-Ni headgroups (DOGS-NTA-Ni), thus imitating ligand-induced ALK

dimerization. This method has been used to promote assembly and activation of other receptor fragments, including EGFR-TKD (22, 23), and dramatically enhances the rate of ALK-TKD autophosphorylation (Fig. 4A).

Our initial investigations with $MnCl_2$-containing assay conditions used in previous ALK-TKD studies (24–26) suggested a mere ~3-fold increase in kinase activity upon autophosphorylation. This contrasts starkly with the ~100–200-fold activity increase typically seen upon activation loop autophosphorylation of other kinases from the insulin receptor (IR) family (27–29). The anomaly arises because the previously used high (non-physiological) Mn^{2+} concentrations both increase unphosphorylated ALK-TKD activity (fig. S3A–C) – as reported for other RTKs (30, 31) – and reduce activity of fully autophosphorylated ALK-TKD (fig. S3D). We therefore used a more physiological 10mM $MgCl_2$ in subsequent studies (and no Mn^{2+}). Under these conditions, autophosphorylation promotes strong ALK-TKD activation (see below), as do the F1174L and R1275Q mutations (Fig 4B, fig. S3E).

Native gel electrophoresis (Fig. 4B) showed that autophosphorylation of dephosphorylated ALK-TKD is substantially accelerated by the F1174L and R1275Q mutations – confirming that these mutations activate the isolated kinase domain. Mobility of ALK-TKD in native gels is increased by autophosphorylation, with successive autophosphorylation events giving rise to four differently phosphorylated species over a period of 0.5 to 20 minutes at 37°C. Whereas unphosphorylated wild-type ALK-TKD was still detectable in Fig. 4B after 4 minutes, this species disappeared completely within 1 minute for both mutated forms. Similarly, the first pALK-TKD species persisted until at least 8 minutes for wild-type protein, but only until ~2 minutes for F1174L ALK-TKD and ~3 minutes for R1275Q ALK-TKD. These results are shown graphically in fig. S4. We ruled out the possibility that increased dimerization of mutated TKDs enhances their autophosphorylation by using analytical ultracentrifugation (fig. S5). ALK-TKD remains monomeric in solution regardless of mutation. The increased ALK-TKD autophosphorylation rates promoted by the F1174L and R1275Q mutations therefore reflect elevated basal kinase activity.

Wild-type and mutated ALK-TKDs have similar inhibitor selectivity profiles

The relative crizotinib resistance of F1174L-mutated ALK observed in cell-based and xenograft studies prompted us to compare its inhibitor selectivity profile with those of wild-type and R1275Q-mutated ALK. We reasoned that the F1174L mutation might alter the drug binding site so that certain ATP-competitive compounds (such as crizotinib) are less effective inhibitors of this variant than of R1275Q or wild-type. To establish inhibitor selectivity profiles for wild-type, F1174L and R1275Q ALK-TKD, we assessed the ability of a panel of 320 well-characterized kinase inhibitors to inhibit their *in vitro* autophosphorylation (see Supplementary Methods). As shown in fig. S6, the inhibition profile of F1174L mutated ALK-TKD was essentially identical to those for wild-type and R1275Q mutated ALK-TKD. Thus, the F1174L mutation does not appear to change the relative abilities of different inhibitors to bind ALK-TKD.

Autophosphorylation alone is sufficient for maximal ALK-TKD activation

To better understand the reduced crizotinib sensitivity of F1174L-mutated ALK, we analyzed kinase activity more quantitatively. As a baseline for these studies, it was important first to establish the full range of wild-type ALK-TKD activity levels – in fully activated and unactivated states respectively. We monitored tyrosine phosphorylation of a peptide corresponding to the ALK activation loop, with sequence ARDIYRASYYRKGGCAMLPVK [‘YYY’ peptide (25)]. Table 1 lists kinetic parameters

(k_{cat}, $K_{m,\ peptide}$, and $K_{m,\ ATP}$) for wild-type ALK-TKD in both inactive (unphosphorylated) and activated (fully autophosphorylated) states.

As shown in Fig. 4C and Table 1, autophosphorylation elevates ALK-TKD catalytic efficiency primarily through a 45-fold increase in k_{cat} ($p < 0.0001$), from 9.32 ± 0.85 min^{-1} (unphosphorylated) to 424 ± 63 min^{-1} (fully phosphorylated), accompanied by a 1.6-fold decrease in $K_{m,\ peptide}$. Values for $K_{m,\ ATP}$ are higher than reported from Mn^{2+}-containing assays (24–26), and are not significantly altered by ALK-TKD autophosphorylation (Table 1; Fig. 4D). This contrasts with other RTKs, where activation loop autophosphorylation reduces K_m for both peptide and ATP substrates under similar ($MnCl_2$-free) assay conditions (28, 29, 32). Unlike other members of its family, ALK therefore does not appear to be autoinhibited by pseudosubstrate-like interaction of its unphosphorylated activation loop with the active site.

Although autophosphorylation clearly increases ALK-TKD activity, we wondered whether TKD dimerization might play an additional allosteric activating role, as seen with EGFR (23). Whereas clustering EGFR-TKD on the surface of vesicles containing DOGS-NTA-Ni lipids promotes significant activation (Fig. 4E), no activating effect was seen when fully phosphorylated pALK-TKD was similarly treated (Fig. 4F). These data argue against an allosteric activation mechanism, and suggest that autophosphorylation is sufficient for maximum ALK activation.

F1174L and R1275Q mutations constitutively activate ALK-TKD, and display different kinetic profiles

As reported in Table 1, the F1174L and R1275Q mutations both cause significant increases in k_{cat} even without autophosphorylation. The F1174L mutation increases k_{cat} by ~40-fold ($p = 0.0013$) to 365 ± 61 min^{-1}: close to the maximum measured for fully phosphorylated wild-type protein. The R1275Q mutation has a more modest effect, increasing k_{cat} of unphosphorylated ALK-TKD by just 12-fold ($p = 0.0001$). Interestingly, whereas the R1275Q mutation leaves $K_{m,\ peptide}$ unaltered, the F1174L mutation increases $K_{m,\ peptide}$ by ~3 fold. These two neuroblastoma mutations therefore promote similar (10-fold) increases in catalytic efficiency ($k_{cat}/K_{m,\ peptide}$) of unphosphorylated ALK-TKD (Fig. 5A, Table 1) in the presence of saturating ATP. Autophosphorylation further increases catalytic efficiency ($k_{cat}/K_{m,\ peptide}$) for both R1275Q and F1174L ALK-TKD variants (Fig. 5E). For R1275Q, this results largely from an increase (~3-fold) in k_{cat}. For F1174L, phosphorylation reduces $K_{m,\ peptide}$ by ~7-fold (Table 1). In addition to being constitutively activated, F1174L ALK-TKD may be slightly ‘superactivated’ upon full autophosphorylation for the particular peptide substrate used here (Fig. 5B), with a catalytic efficiency that is ~30% higher than measured for WT ($p = 0.0342$) or R1275Q ($p = 0.0327$) pALK-TKD.

Reduced K_m for ATP explains the relative resistance of F1174L-mutated ALK to crizotinib

The $K_{m,\ ATP}$ values listed in Table 1 (and Fig. 5C) suggest one explanation for the reduced crizotinib sensitivity of cell-lines and xenografts expressing F1174L-mutated ALK. $K_{m,\ ATP}$ for the F1174L mutant is 2.3-fold lower than that of R1275Q ($p = 0.0007$) when autophosphorylated (Fig. 5D,F), and 2.6-fold lower ($p = 0.0045$) in the dephosphorylated form (Fig. 5C,F). This trend was maintained when the assay was repeated at a higher peptide concentration of 2mM (fig. S7, table S2). These data suggest that the F1174L mutation enhances the ATP-binding affinity of ALK, which in turn will reduce potency of any ATP binding site competitor (such as crizotinib) at cellular ATP concentrations – as seen for drug-resistance mutations in other RTKs (33).

To test this hypothesis, we compared the *in vitro* crizotinib sensitivity of the recombinant ALK-TKD variants at two different ATP concentrations (Fig. 5G,H). At 0.2mM ATP (significantly lower than cellular levels) IC_{50} values (measured for 50nM unphosphorylated protein) were similar for R1275Q and F1174L ALK-TKD (Fig. 5G, table S3). However, at a more physiological ATP concentration of 2mM, F1174L ALK-TKD was significantly less sensitive ($p = 0.0128$) to crizotinib inhibition (IC_{50} = 130nM) than R1275Q ALK-TKD (IC_{50} = 84.6nM). A similar difference was also seen with autophosphorylated proteins (table S4), as anticipated from Table 1. Wild-type ALK-TKD resembled the F1174L variant in its relative insensitivity to crizotinib inhibition *in vitro* (table S3, S4), consistent with the finding that the drug does not inhibit growth of neuroblastoma cells that express wild-type ALK at normal levels (Figs. 1B & 2E). However, NB1 cells that express the receptor at very high levels because of an ALK amplification are sensitive to crizotinib (Figs. 1B & 2D), indicating that inhibitor response may also be affected by issues of trafficking, subcellular localization, and expression level (19).

The correlation between the increased ATP-binding affinity of F1174L-mutated ALK and its reduced sensitivity to crizotinib argues that this effect will be general – affecting the response to all ATP-competitive inhibitors. We tested this hypothesis with two other inhibitors. As shown in fig. S8 and table S5, *in vitro* inhibition of ALK-TKD by staurosporine is also impaired by the F1174L mutation compared with that seen for R1275Q-mutated ALK-TKD. Moreover, the ALK/IGF1-R/IR inhibitor GSK1838705A (34), is substantially less effective at inducing cytotoxicity in neuroblastoma cell lines expressing F1174L ALK than those expressing R1275Q ALK (table S6). Like crizotinib, GSK1838705A only showed significant *in vivo* activity against R1275Q xenografts (fig. S9). These data, and the $K_{m,\,ATP}$ values reported in Table 1, therefore suggest that F1174L-mutated ALK will be less sensitive to all ATP-competitive inhibitors.

Structural basis for increased ATP-binding affinity in F1174L-mutated ALK

Recent crystal structures of ALK-TKD (24, 26) revealed unexpected similarities with EGFR-TKD that are useful for understanding and predicting the consequences of ALK mutations. In the inactive ALK and EGFR TKD structures, key autoinhibitory interactions between the crucial αC-helix and a short α-helix at the beginning of the activation loop (magenta in Fig. 6) displace the αC-helix from the position it must adopt in the 'active' kinase. Intriguingly, the location of R1275 in ALK coincides very closely with that of L837 in EGFR (L861 in pro-EGFR), where mutation to glutamine activates EGFR in NSCLC (35). The R1275 side-chain contributes directly to interactions between the magenta activation loop helix and the αC-helix (Fig. 6B), stabilizing the autoinhibited ALK-TKD conformation. Replacing R1275 with a glutamine, or phosphorylating nearby Y1278 in the activation loop (Fig 6B), will disrupt these autoinhibitory interactions and thus activate ALK.

F1174 lies at the C-terminus of the αC-helix (Fig. 6B), and its side-chain contributes to the small well-packed hydrophobic 'core' between αC and the activation loop. A reduction in the size of the F1174 side-chain will disrupt this packing, weakening autoinhibitory interactions and thus allowing ALK-TKD to adopt its active configuration. F1174 also makes another important interaction that may explain its effects on ATP binding. As shown in Fig. 6C, F1174 is in direct van der Waal's contact with F1271 of the crucial 'DFG' motif, the aspartate of which (D1270) coordinates a Mg^{2+} ion involved in ATP binding. Reducing the size of the F1174 side chain would remove one structural restraint on the DFG motif, which may allow D1270 to adopt a position with more optimal Mg^{2+}-coordination geometry – slightly increasing ATP-binding affinity (*i.e.* reducing $K_{m,\,ATP}$). By contrast, crizotinib makes no interactions with the DFG motif (Fig. 6C, lower panel), and does not come within 4Å of the D1270 side-chain – so altering the DFG motif position should not affect crizotinib

binding. These observations provide a structural hypothesis for how the F1174L mutation can increase the affinity of ALK-TKD for ATP without affecting its affinity for ATP-competitive inhibitors such as crizotinib, staurosporine, and GSK1838705A – leading to relative resistance. By contrast, the R1275 side chain is more than 7Å away from the ATP-binding site, so its mutation should not directly affect ATP binding.

DISCUSSION

Genetic studies have firmly established ALK as a tractable molecular target in neuroblastoma, as well as several other human malignancies including NSCLC. We establish here that neuroblastoma cell lines driven by ALK mutation or amplification are sensitive to crizotinib, an orally bioavailable ATP-competitive ALK inhibitor. Neuroblastoma cell lines and xenografts that express R1275Q-ALK, one of the two most commonly occurring mutations (12), are highly sensitive to crizotinib. By contrast, those expressing F1174L-mutated ALK (the other of the two most common mutations) are resistant to crizotinib *in vitro* and *in vivo*. We show that the reduced sensitivity of F1174L-expressing cell lines can be explained, at least in part, by an increased ATP-binding affinity compared with R1275Q – as manifest by $K_{m,\ ATP}$ values – and this reduces potency of several ATP-competitive inhibitors.

The R1275Q mutation in ALK resembles oncogenic EGFR mutations found in NSCLC, such as L834R (L858R in pro-EGFR), increasing both k_{cat} and $K_{m,\ ATP}$ (36, 37). By contrast, the F1174L mutation in ALK appears to combine the characteristics of an activating mutation and a resistance mutation – increasing k_{cat} while maintaining a wild-type-like $K_{m,\ ATP}$. The F1174L mutation thus resembles the drug-resistant EGFR L834R/T766M double mutation (L858R/T790M in pro-EGFR) that has a reduced $K_{m,\ ATP}$ (33, 37). Interestingly, the F1174L mutation has emerged not only as a built-in resistance mechanism in neuroblastoma as described here, but also as an escape mechanism in ALK-translocated tumors treated with crizotinib (17).

Despite the resistance described here, our results indicate that patients harboring the F1174L ALK mutation may benefit from treatment with ATP-competitive ALK inhibitors in some circumstances. For crizotinib itself, an increase in dosage to overcome the relative difference in $K_{m,\ ATP}$ compared with R1275Q-mutated ALK may be possible – although it remains unclear whether the exposures necessary to achieve the biochemical effect in tumor tissue will be achievable in the clinic. Crizotinib was well tolerated in adult patients with refractory lung cancer (15), suggesting that a therapeutic window exists, and that pediatric phase 1 studies should seek to define a true maximum tolerated dose in an effort to circumvent the *de novo* resistance caused by the F1174L mutation. The absence of an appropriate active site cysteine precludes the irreversible inhibitor approach being investigated for EGFR (38). Alternative strategies include use of therapeutic ALK antibody reagents for patients whose tumors harbor the F1174L mutation, and/or developing ATP-competitive inhibitors that can overcome the $K_{m,\ ATP}$ effects by having higher affinity for ALK while retaining selectivity.

MATERIALS AND METHODS

In vitro tumor growth inhibition

In vitro crizotinib activity was evaluated in 18 neuroblastoma cell lines using the real-time cell electronic sensing (RT-CES) system (ACEA Biosciences, San Diego, CA). Cell lines were plated at 5,000 – 30,000 cells per well depending on growth kinetics, and drug was added at 1–10,000nM after 24h. IC_{50} was calculated from the cell index in triplicate samples after 72h of incubation. Growth inhibition at 333nM crizotinib was calculated using the formula: % Inhibition = 100 × (Cell index control – cell index treatment)/Cell index control.

Due to non-comparable maximum growth inhibition depending on ALK status, growth inhibition at a single pharmacologically relevant dose was used to compare cell lines. *p* values were calculated using two sided exact Wilcoxon-Mann-Whitney tests. All lines were routinely mycoplasma tested and genotyped (AmpFLSTR Identifiler kit; Applied Biosystems) to verify identity.

In vitro protein and phosphoprotein detection

Each cell line was grown to 70–80% confluence, treated with crizotinib at the noted concentration (ranging from 0 to 10,000nM) for 2h, and washed twice with ice cold PBS. Whole cell lysates were then analyzed by immunoblotting as described (7), using anti-ALK (1:1,000; Cell Signaling, 3333), anti-phospho-ALK Tyr 1604 (1:1,000, Cell Signaling, 3341), anti-actin (1:2,000; Santa Cruz, sc-1616). Immunoblot quantitation employed ImageJ (NIH).

In vivo tumor growth inhibition

CB17 *scid* female mice (Taconic Farms, NY) were used to propagate subcutaneously implanted neuroblastoma tumors. Tumor diameters were measured twice per week using electronic calipers, and tumor volumes calculated using the spheroid formula, $(\Pi/6)*d^3$, where d represents mean diameter. Once tumor volume exceeded $200mm^3$, mice were randomized (n=10 per arm) to receive crizotinib (100mg/kg/dose) or vehicle (acidified water) daily by oral gavage for four weeks. Mice were maintained under protocols and conditions approved by our institutional animal care and use committee. Mice were sacrificed when tumor volume exceeded $1500mm^3$. A mixed-effects linear model was used to assess tumor volume over time between treatment and vehicle groups, controlling for tumor size at enrollment. Survival analysis was performed using the Log-Rank test with progression defined as tumor volume exceeding $1500mm^3$ or treatment-related death.

In vivo protein and phosphoprotein detection

Mice harboring subcutaneously implanted NB1643 neuroblastoma tumors were randomized once tumor volume exceeded 300 mm^3 (n=3 per arm) to receive crizotinib or vehicle as described above for 2 days. Mice were sacrificed 4 hours after the final dose, tumors were immediately snap frozen in liquid nitrogen, and pulverized for extraction of whole cell lysates using 100µl extraction buffer (FNN011, Invitrogen) containing protease inhibitor (P-2714, Sigma), phosphatase inhibitors (P-5726, Sigma) and phenylmethyl sulfonyl fluoride. Lysates were sonicated, rotated for 1h at 4°C, and clarified by centrifugation. Protein concentration was normalized using the Bradford method, and lysates (200µg) were subjected to immunoblotting as outlined above.

Recombinant protein expression and purification

A construct encoding ALK residues 1090–1416, together with an N-terminal hexahistidine tag, was used to express histidine-tagged recombinant ALK-TKDs in Sf9 cells as described in Supplementary Methods.

Native gel kinase assays

Native gel electrophoresis was used to monitor autophosphorylation progress for 10µM ALK-TKD in 100mM HEPES pH 7.4, 150mM NaCl, 2mM DTT, 2mM ATP, 10mM $MgCl_2$, either free in solution or in the presence of lipid vesicles containing 10% DOGS-NTA-Ni (100µM total lipid). Aliquots (10µl) were taken at each time point, quenched by adding EDTA to 20mM and placing on ice, and then subjected to electrophoresis on 7.5% Tris-glycine native gels at 100V for ~14 hours. Gels were stained with Coomassie brilliant blue R-250.

Peptide phosphorylation assays

Analysis of substrate phosphorylation by ALK-TKD employed a peptide mimic of the ALK activation loop with sequence: biotin-ARDIYRASYYRKGGCAMLPVK (CanPeptide), referred to as YYY peptide (25). Assay details (with Mg^{2+} as divalent cation) and analysis of inhibition are described in Supplementary Methods. Spontaneous autophosphorylation is negligible at the ALK-TKD concentrations used for assays.

Supplementary Material

Refer to Web version on PubMed Central for supplementary material.

Acknowledgments

We thank members of the Lemmon, Mossé and Maris laboratories for valuable discussions, and Pfizer for their gift of crizotinib.

Funding: This work was funded in part by the U.S. Army Peer-Reviewed Medical Research Program (W81XWH-10-1-0212/3 to M.A.L./Y.P.M.), NIH Grant R01-CA140198 (Y.P.M.), the Carly Hillman Fund (Y.P.M.), the Alex's Lemonade Stand Foundation (J.M.M.), and the Abramson Family Cancer Research Institute (J.M.M.). S.C.B. was supported by an NIH Training Grant in Structural Biology (T32-GM008275). A.C.W. was supported by a fellowship from the St. Baldrick's Foundation.

REFERENCES AND NOTES

1. D'Angio GJ, Evans AE, Koop CE. Special pattern of widespread neuroblastoma with a favourable prognosis. Lancet. 1971; 1:1046–1049. [PubMed: 4102970]
2. Hobbie WL, Moshang T, Carlson CA, Goldmuntz E, Sacks N, Goldfarb SB, Grupp SA, Ginsberg JP. Late effects in survivors of tandem peripheral blood stem cell transplant for high-risk neuroblastoma. Pediatr. Blood Cancer. 2008; 51:679–683. [PubMed: 18623215]
3. Iwahara T, Fujimoto J, Wen D, Cupples R, Bucay N, Arakawa T, Mori S, Ratzkin B, Yamamoto T. Molecular characterization of ALK, a receptor tyrosine kinase expressed specifically in the nervous system. Oncogene. 1997; 14:439–449. [PubMed: 9053841]
4. Morris SW, Kirstein MN, Valentine MB, Dittmer KG, Shapiro DN, Saltman DL, Look AT. Fusion of a kinase gene, ALK, to a nucleolar protein gene, NPM, in non-Hodgkin's lymphoma. Science. 1994; 263:1281–1284. [PubMed: 8122112]
5. Soda M, Choi YL, Enomoto M, Takada S, Yamashita Y, Ishikawa S, Fujiwara S, Watanabe H, Kurashina K, Hatanaka H, Bando M, Ohno S, Ishikawa Y, Aburatani H, Niki T, Sohara Y, Sugiyama Y, Mano H. Identification of the transforming EML4-ALK fusion gene in non-small-cell lung cancer. Nature. 2007; 448:561–566. [PubMed: 17625570]
6. Palmer RH, Vernersson E, Grabbe C, Hallberg B. Anaplastic lymphoma kinase: signalling in development and disease. Biochem. J. 2009; 420:345–361. [PubMed: 19459784]
7. Mossé YP, Laudenslager M, Longo L, Cole KA, Wood A, Attiyeh EF, Laquaglia MJ, Sennett R, Lynch JE, Perri P, Laureys G, Speleman F, Kim C, Hou C, Hakonarson H, Torkamani A, Schork NJ, Brodeur GM, Tonini GP, Rappaport E, Devoto M, Maris JM. Identification of ALK as a major familial neuroblastoma predisposition gene. Nature. 2008; 455:930–935. [PubMed: 18724359]
8. Carén H, Abel F, Kogner P, Martinsson T. High incidence of DNA mutations and gene amplifications of the ALK gene in advanced sporadic neuroblastoma tumours. Biochem. J. 2008; 416:153–159. [PubMed: 18990089]
9. Chen Y, Takita J, Choi YL, Kato M, Ohira M, Sanada M, Wang L, Soda M, Kikuchi A, Igarashi T, Nakagawara A, Hayashi Y, Mano H, Ogawa S. Oncogenic mutations of ALK kinase in neuroblastoma. Nature. 2008; 455:971–974. [PubMed: 18923524]
10. George RE, Sanda T, Hanna M, Frohling S, Luther W 2nd, Zhang J, Ahn Y, Zhou W, London WB, McGrady P, Xue L, Zozulya S, Gregor VE, Webb TR, Gray NS, Gilliland DG, Diller L, Greulich H, Morris SW, Meyerson M, Look AT. Activating mutations in ALK provide a therapeutic target in neuroblastoma. Nature. 2008; 455:975–978. [PubMed: 18923525]

11. Janoueix-Lerosey I, Lequin D, Brugieres L, Ribeiro A, de Pontual L, Combaret V, Raynal V, Puisieux A, Schleiermacher G, Pierron G, Valteau-Couanet D, Frebourg T, Michon J, Lyonnet S, Amiel J, Delattre O. Somatic and germline activating mutations of the ALK kinase receptor in neuroblastoma. Nature. 2008; 455:967–970. [PubMed: 18923523]
12. De Brouwer S, De Preter K, Kumps C, Zabrocki P, Porcu M, Westerhout EM, Lakeman A, Vandesompele J, Hoebeeck J, Van Maerken T, De Paepe A, Laureys G, Schulte JH, Schramm A, Van Den Broecke C, Vermeulen J, Van Roy N, Beiske K, Renard M, Noguera R, Delattre O, Janoueix-Lerosey I, Kogner P, Martinsson T, Nakagawara A, Ohira M, Caron H, Eggert A, Cools J, Versteeg R, Speleman F. Meta-analysis of neuroblastomas reveals a skewed ALK mutation spectrum in tumors with MYCN amplification. Clin. Cancer Res. 2010; 16:4354–4363.
13. Murugan AK, Xing M. Novel oncogenic mutations of the ALK gene in anaplastic thyroid cancer. Cancer Res. 2011; 71:4403–4411. [PubMed: 21596819]
14. Christensen JG, Zou HY, Arango ME, Li Q, Lee JH, McDonnell SR, Yamazaki S, Alton GR, Mroczkowski B, Los G. Cytoreductive antitumor activity of PF-2341066, a novel inhibitor of anaplastic lymphoma kinase and c-Met, in experimental models of anaplastic large-cell lymphoma. Mol. Cancer Ther. 2007; 6:3314–3322. [PubMed: 18089725]
15. Kwak EL, Bang YJ, Camidge DR, Shaw AT, Solomon B, Maki RG, Ou SH, Dezube BJ, Janne PA, Costa DB, Varella-Garcia M, Kim WH, Lynch TJ, Fidias P, Stubbs H, Engelman JA, Sequist LV, Tan W, Gandhi L, Mino-Kenudson M, Wei GC, Shreeve SM, Ratain MJ, Settleman J, Christensen JG, Haber DA, Wilner K, Salgia R, Shapiro GI, Clark JW, Iafrate AJ. Anaplastic lymphoma kinase inhibition in non-small-cell lung cancer. N. Engl. J. Med. 2010; 363:1693–1703. [PubMed: 20979469]
16. Choi YL, Soda M, Yamashita Y, Ueno T, Takashima J, Nakajima T, Yatabe Y, Takeuchi K, Hamada T, Haruta H, Ishikawa Y, Kimura H, Mitsudomi T, Tanio Y, Mano H. ALK Lung Cancer Study Group. EML4-ALK mutations in lung cancer that confer resistance to ALK inhibitors. N. Engl. J. Med. 2010; 363:1734–1739. [PubMed: 20979473]
17. Sasaki T, Okuda K, Zheng W, Butrynski J, Capelletti M, Wang L, Gray NS, Wilner K, Christensen JG, Demetri G, Shapiro GI, Rodig SJ, Eck MJ, Janne PA. The neuroblastoma associated F1174L ALK mutation causes resistance to an ALK kinase inhibitor in ALK translocated cancers. Cancer Res. 2010; 70:10038–10043. [PubMed: 21030459]
18. Katayama R, Khan TM, Benes C, Lifshits E, Ebi H, Rivera VM, Shakespeare WC, Iafrate AJ, Engelman JA, Shaw AT. Therapeutic strategies to overcome crizotinib resistance in non-small cell lung cancers harboring the fusion oncogene EML4-ALK. Proc. Natl. Acad. Sci. U.S.A. 2011; 108:7535–7540. [PubMed: 21502504]
19. Mazot P, Cazes A, Boutterin MC, Figueiredo A, Raynal V, Combaret V, Hallberg B, Palmer RH, Delattre O, Janoueix-Lerosey I, Vigny M. The constitutive activity of the ALK mutated at positions F1174 or R1275 impairs receptor trafficking. Oncogene. 2011; 30:2017–2025. [PubMed: 21242967]
20. Martinsson T, Eriksson T, Abrahamsson J, Caren H, Hansson M, Kogner P, Kamaraj S, Schönherr C, Weinmar J, Ruuth K, Palmer RH, Hallberg B. Appearance of the novel activating F1174S ALK mutation in neuroblastoma correlates with aggressive tumor progression and unresponsiveness to therapy. Cancer Res. 2011; 71:98–105. [PubMed: 21059859]
21. Moog-Lutz C, Degoutin J, Gouzi JY, Frobert Y, Brunet-de Carvalho N, Bureau J, Créminon C, Vigny M. Activation and inhibition of anaplastic lymphoma kinase receptor tyrosine kinase by monoclonal antibodies and absence of agonist activity of pleiotrophin. J. Biol. Chem. 2005; 280:26039–26048. [PubMed: 15886198]
22. Shrout AL, Montefusco DJ, Weis RM. Template-directed assembly of receptor signaling complexes. Biochemistry. 2003; 42:13379–13385. [PubMed: 14621982]
23. Zhang X, Gureasko J, Shen K, Cole PA, Kuriyan J. An allosteric mechanism for activation of the kinase domain of epidermal growth factor receptor. Cell. 2006; 125:1137–1149. [PubMed: 16777603]
24. Bossi RT, Saccardo MB, Ardini E, Menichincheri M, Rusconi L, Magnaghi P, Orsini P, Avanzi N, Borgia AL, Nesi M, Bandiera T, Fogliatto G, Bertrand JA. Crystal structures of anaplastic lymphoma kinase in complex with ATP competitive inhibitors. Biochemistry. 2010; 49:6813–6825. [PubMed: 20695522]

25. Donella-Deana A, Marin O, Cesaro L, Gunby RH, Ferrarese A, Coluccia AM, Tartari CJ, Mologni L, Scapozza L, Gambacorti-Passerini C, Pinna LA. Unique substrate specificity of anaplastic lymphoma kinase (ALK): development of phosphoacceptor peptides for the assay of ALK activity. Biochemistry. 2005; 44:8533–8542. [PubMed: 15938644]
26. Lee CC, Jia Y, Li N, Sun X, Ng K, Ambing E, Gao MY, Hua S, Chen C, Kim S, Michellys PY, Lesley SA, Harris JL, Spraggon G. Crystal structure of the ALK (anaplastic lymphoma kinase) catalytic domain. Biochem. J. 2010; 430:425–437. [PubMed: 20632993]
27. Cobb MH, Sang BC, Gonzalez R, Goldsmith E, Ellis L. Autophosphorylation activates the soluble cytoplasmic domain of the insulin receptor in an intermolecular reaction. J. Biol. Chem. 1989; 264:18701–18706. [PubMed: 2808393]
28. Favelyukis S, Till JH, Hubbard SR, Miller WT. Structure and autoregulation of the insulin-like growth factor 1 receptor kinase. Nat. Struct. Mol. Biol. 2001; 8:1058–1063.
29. Furdui CM, Lew ED, Schlessinger J, Anderson KS. Autophosphorylation of FGFR1 kinase is mediated by a sequential and precisely ordered reaction. Mol. Cell. 2006; 21:711–717. [PubMed: 16507368]
30. Grace MR, Walsh CT, Cole PA. Divalent ion effects and insights into the catalytic mechanism of protein tyrosine kinase Csk. Biochemistry. 1997; 36:1874–1881. [PubMed: 9048573]
31. Wente SR, Villalba M, Schramm VL, Rosen OM. Mn2(+)-binding properties of a recombinant protein-tyrosine kinase derived from the human insulin receptor. Proc. Natl. Acad. Sci. U.S.A. 1990; 87:2805–2809. [PubMed: 2157215]
32. Till JH, Becerra M, Watty A, Lu Y, Ma Y, Neubert TA, Burden SJ, Hubbard SR. Crystal structure of the MuSK tyrosine kinase: insights into receptor autoregulation. Structure. 2002; 10:1187–1196. [PubMed: 12220490]
33. Eck MJ, Yun CH. Structural and mechanistic underpinnings of the differential drug sensitivity of EGFR mutations in non-small cell lung cancer. Biochim. Biophys. Acta. 2010; 1804:559–566. [PubMed: 20026433]
34. Sabbatini P, Korenchuk S, Rowand JL, Groy A, Liu Q, Leperi D, Atkins C, Dumble M, Yang J, Anderson K, Kruger RG, Gontarek RR, Maksimchuk KR, Suravajjala S, Lapierre RR, Shotwell JB, Wilson JW, Chamberlain SD, Rabindran SK, Kumar R. GSK1838705A inhibits the insulin-like growth factor-1 receptor and anaplastic lymphoma kinase and shows antitumor activity in experimental models of human cancers. Mol. Cancer Ther. 2009; 8:2811–2820. [PubMed: 19825801]
35. Sharma SV, Bell DW, Settleman J, Haber DA. Epidermal growth factor receptor mutations in lung cancer. Nat. Rev. Cancer. 2007; 7:169–181. [PubMed: 17318210]
36. Carey KD, Garton AJ, Romero MS, Kahler J, Thomson S, Ross S, Park F, Haley JD, Gibson N, Sliwkowski MX. Kinetic analysis of epidermal growth factor receptor somatic mutant proteins shows increased sensitivity to the epidermal growth factor receptor tyrosine kinase inhibitor, erlotinib. Cancer Res. 2006; 66:8163–8171. [PubMed: 16912195]
37. Yun CH, Mengwasser KE, Toms AV, Woo MS, Greulich H, Wong KK, Meyerson M, Eck MJ. The T790M mutation in EGFR kinase causes drug resistance by increasing the affinity for ATP. Proc. Natl. Acad. Sci. U.S.A. 2008; 105:2070–2075. [PubMed: 18227510]
38. Zhou W, Ercan D, Chen L, Yun CH, Li D, Capelletti M, Cortot AB, Chirieac L, Iacob RE, Padera R, Engen JR, Wong KK, Eck MJ, Gray NS, Jänne PA. Novel mutant-selective EGFR kinase inhibitors against EGFR T790M. Nature. 2009; 462:1070–1074. [PubMed: 20033049]

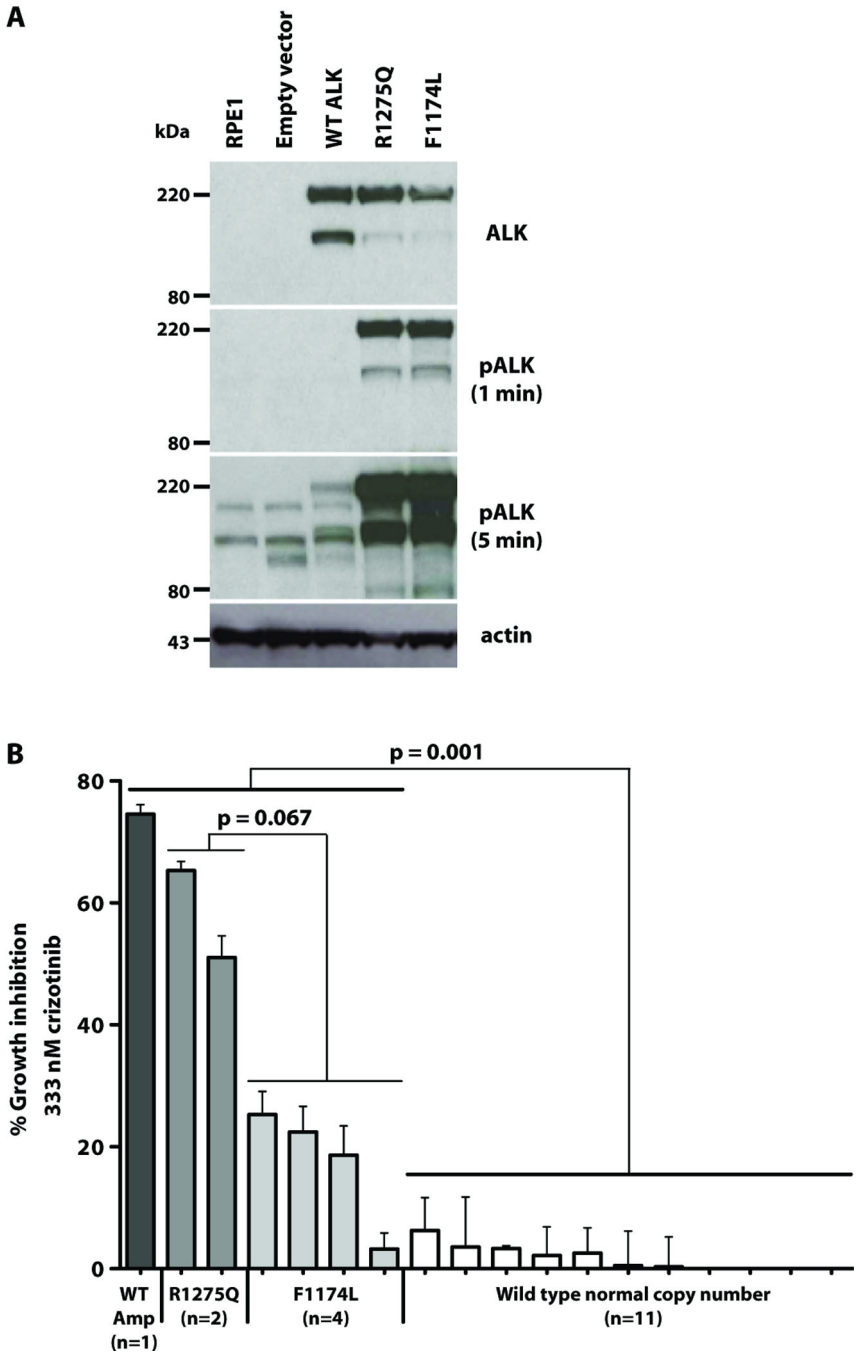

Fig. 1. Constitutive activity and inhibitor sensitivity of F1174L and R1275 ALK mutants

(**A**) Immunoblots of total ALK and pALK in hTERT-RPE1 cells infected with retroviruses directing expression of wild-type or mutated ALK. Lower panel is actin loading control. (**B**) Proliferation of neuroblastoma cell lines over 72 hours of incubation with 333nM crizotinib. Growth inhibition ± S.D. is reported for at least three independent experiments. *p* values were calculated for marked comparisons using two-sided exact Wilcoxon-Mann-Whitney tests. Cell lines were (left to right): wild-type ALK amplified (NB1); R1275Q (NB1643, LAN5); F1174L (SH-SY5Y, KELLY, NBSD, SMS-SAN); wild-type ALK, normal copy number (NB1691, NB-EBc1, IMR5, NB16, NLF, IMR32, NBLS, SKNBE2C, NGP, SKNAS, SKNFI).

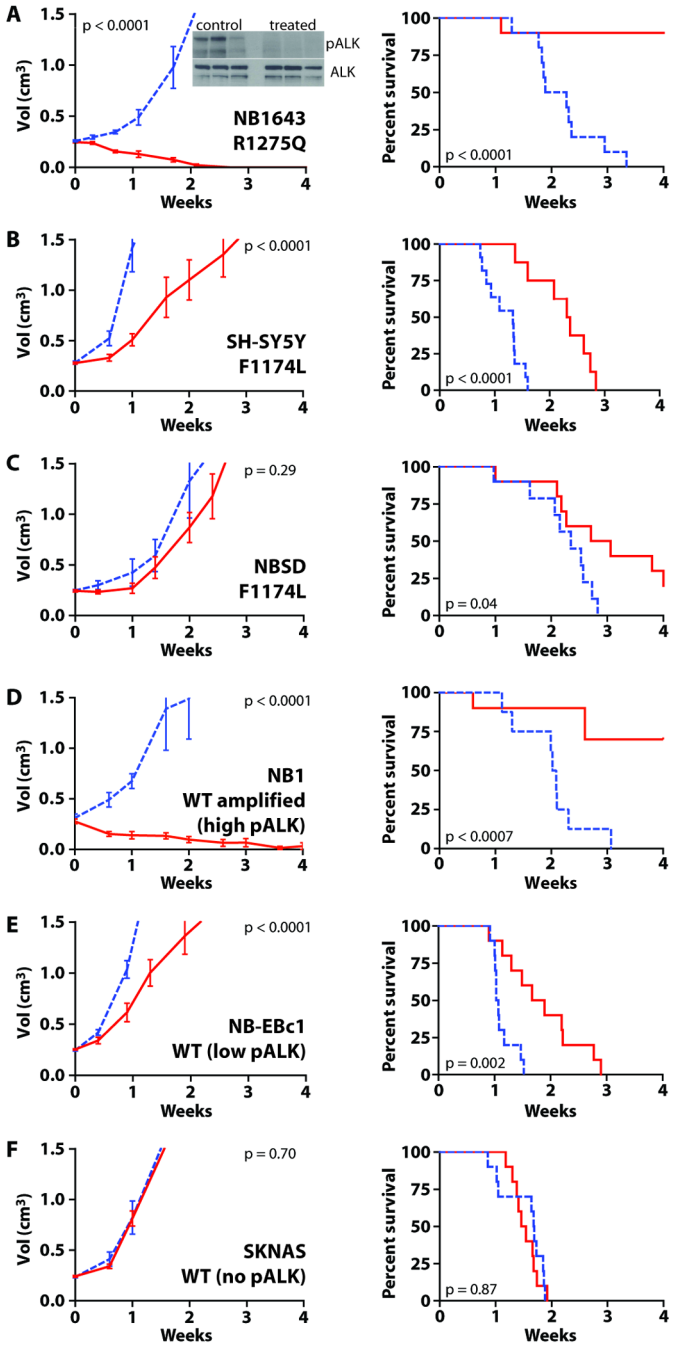

Fig. 2. Crizotinib activity *in vivo* for wild-type and mutated ALK

Subcutaneously implanted neuroblastoma tumors were monitored in CB17 *scid* mice treated with crizotinib (solid red lines), or vehicle (dashed blue lines). Tumor volume (left panels) is displayed as mean ± S.E.M. Study end points for survival analysis (right panels) were tumor volume ≥1.5cm^3 or treatment-related death. (**A**) NB1643 (R1275Q) xenografts: inset shows immunoblot of ALK and pALK; (**B**) SH-SY5Y (F1174L); (**C**) NBSD (F1174L); (**D**) NB1 (wild-type amplified with strong phospho-ALK staining); (**E**) NB-EBc1 (wild-type, with weak phospho-ALK staining); (**F**) SKNAS (wild-type, undetectable pALK). Statistical treatment is described in Materials and Methods.

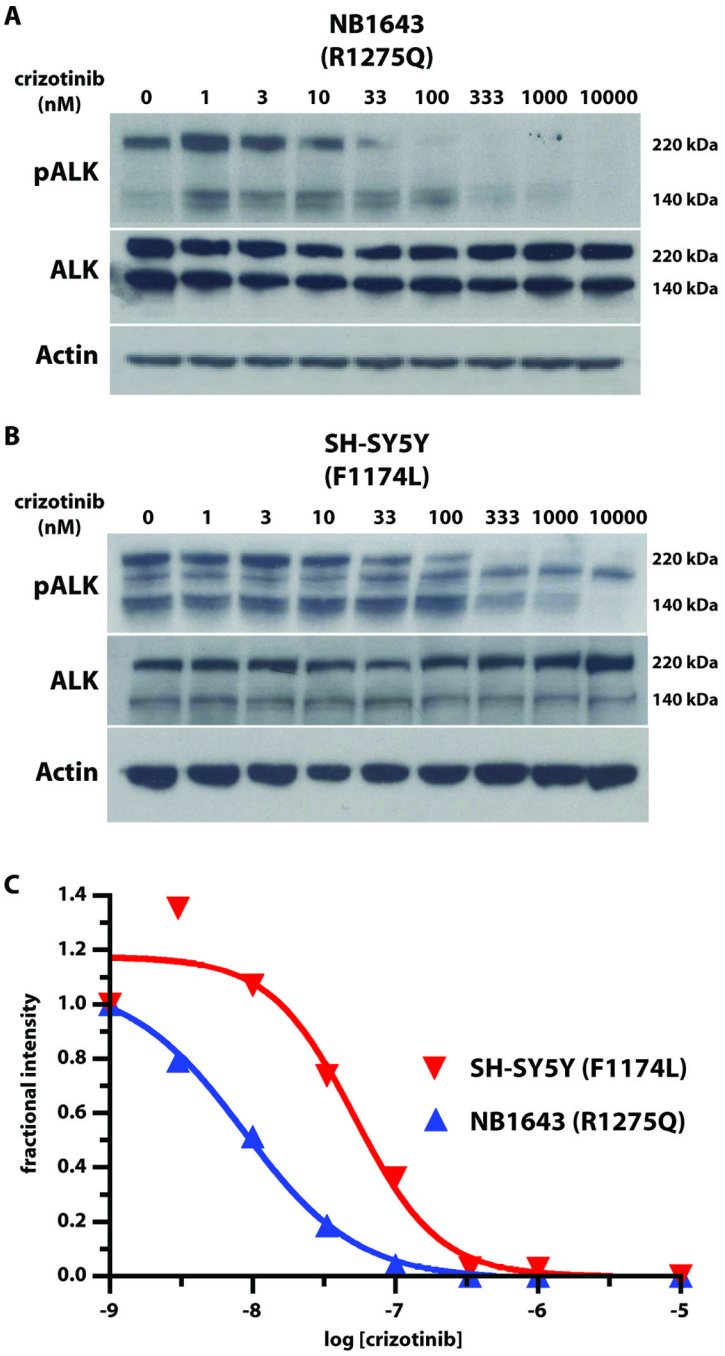

Fig. 3. Inhibition of constitutive ALK autophosphorylation by crizotinib

Representative immunoblots of ALK autophosphorylation in neuroblastoma cell-lines after treatment with different crizotinib concentrations (0 to 10μM). Whole cell lysates were immunoblotted for phospho-ALK (using pY1604 antibody), total ALK, and actin (loading control) for (**A**) NB1643 cells (R1275Q ALK), (**B**) SH-SY5Y cells (F1174L ALK). Downstream signaling molecules are analyzed in fig. S2. (**C**) Quantitation of phospho-ALK levels (220kDa species) as a function of crizotinib concentration.

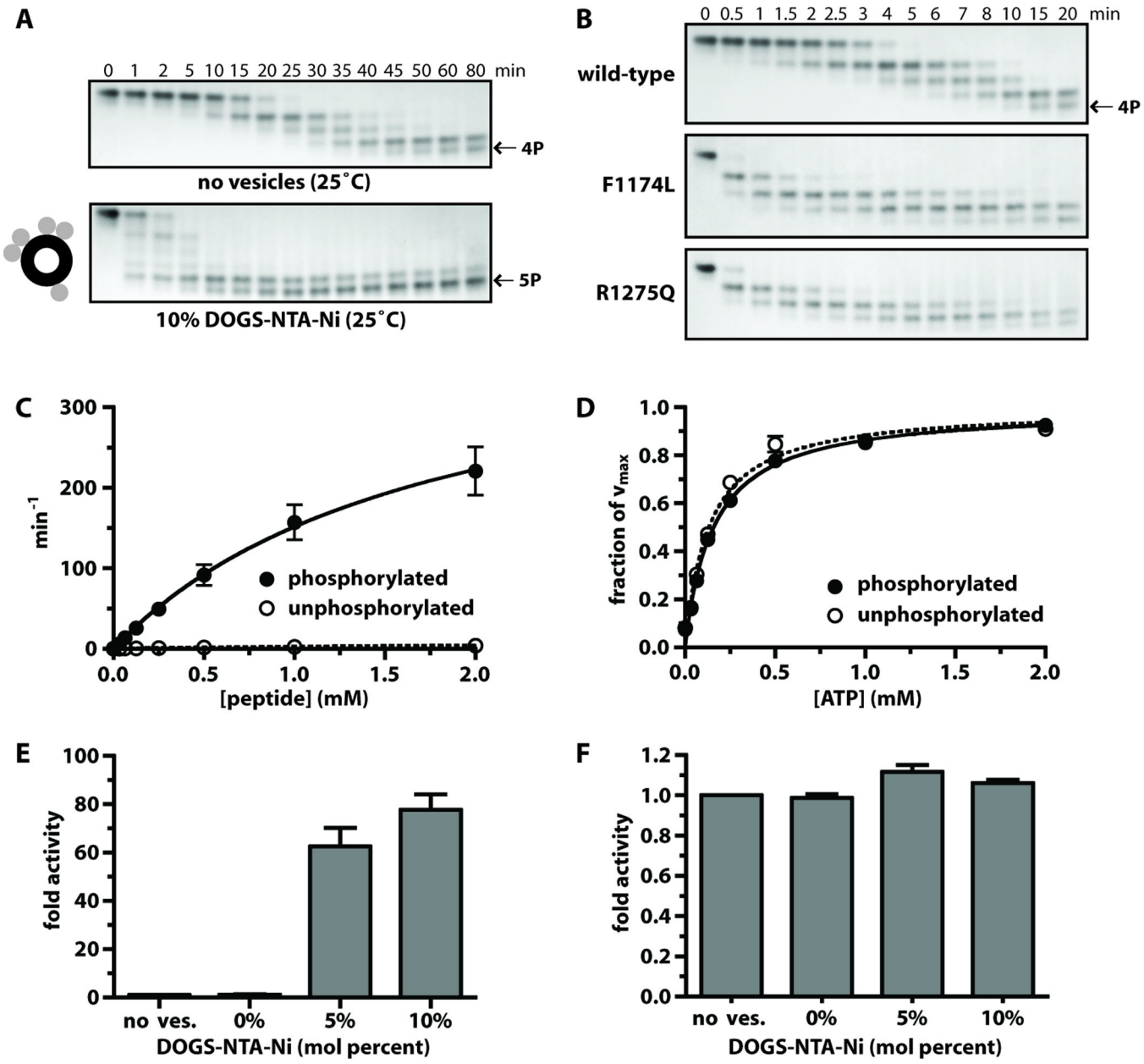

Fig. 4. Analysis of ALK-TKD activation *in vitro*

(**A**) Separation of differently autophosphorylated ALK-TKD species by native gel electrophoresis to monitor autophosphorylation at 25°C in the absence (top) and presence (bottom) of vesicles containing 10% DOGS-NTA-Ni (100μM total lipid), 10mM $MgCl_2$, and 2mM ATP. (**B**) Autophosphorylation of wild-type and mutated ALK-TKD (10μM) with saturating ATP (2mM) and 10mM $MgCl_2$ at 37°C. Results are quantitated in fig. S4. (**C**) Rate of ^{32}P incorporation at 25°C into substrate peptide (see Materials and Methods) for autophosphorylated ALK-TKD (10nM) and unphosphorylated ALK-TKD (500nM) as peptide substrate concentration is increased. ATP concentration was 2mM. (**D**) $K_{m,\ ATP}$ determination for autophosphorylated (10nM) and unphosphorylated (500nM) ALK-TKD at fixed peptide substrate concentration (1mM). (**E**) Enhancement of EGFR-TKD kinase (1μM) by vesicles containing increasing mole percentages of DOGS-NTA-Ni (10μM DOGS-NTA-Ni, 100–200μM total lipid). (**F**) Effect on autophosphorylated ALK-TKD

(1μM) activity of adding DOGS-NTA-Ni vesicles. Data are shown as means ± SEM from at least three independent experiments. All experiments except those in (**B**) were performed at 25°C.

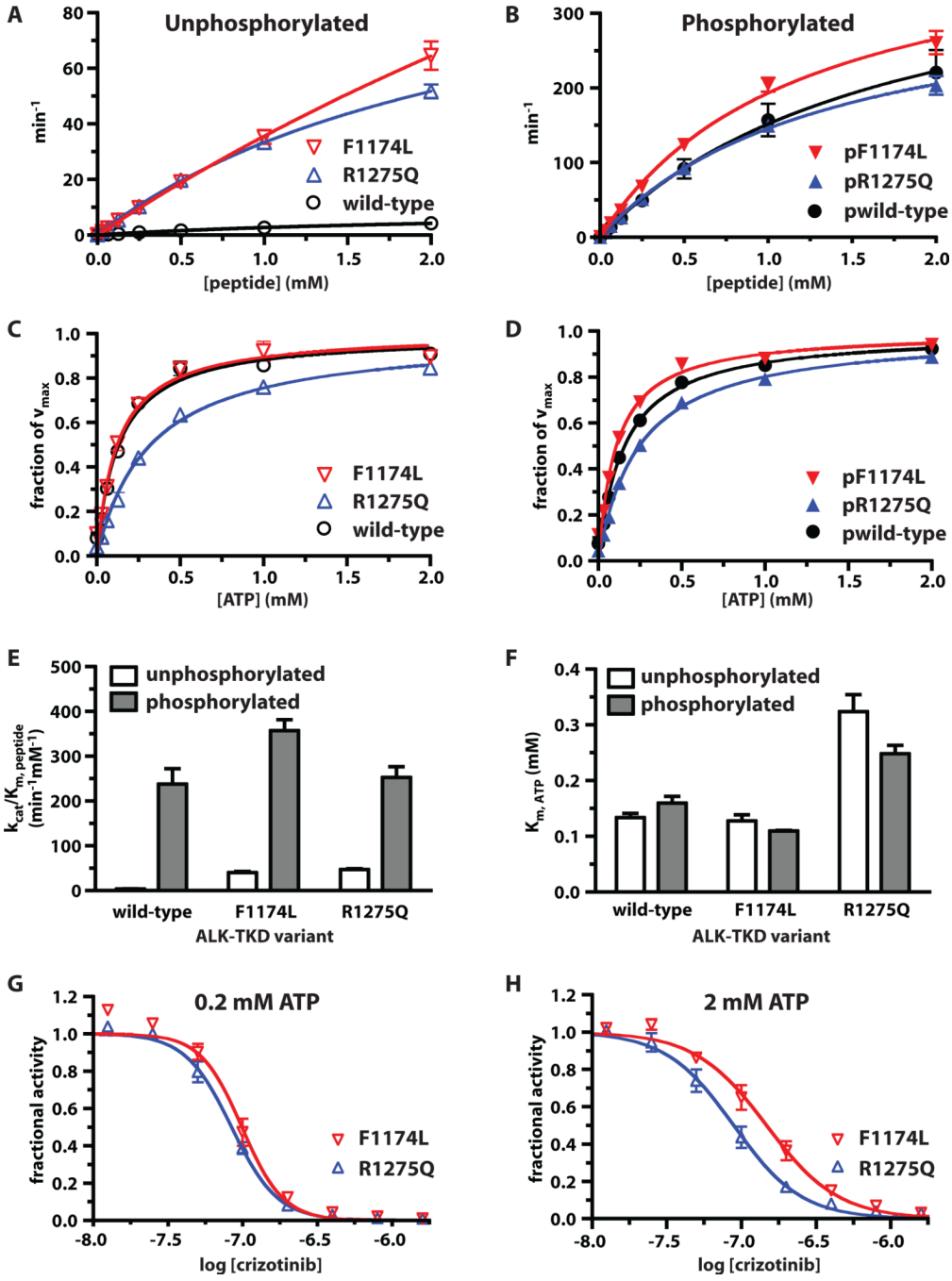

Fig. 5. Comparison of wild-type ALK-TKD with F1174L and R1275Q variants *in vitro*

(**A,B**) Rates of ^{32}P incorporation into 'YYY' peptide at saturating ATP (2mM) for: (**A**) unphosphorylated wild-type (500nM) or mutated (50nM) ALK-TKD; and (**B**) phosphorylated wild-type and mutated ALK-TKD (all at 10nM). (**C,D**) $K_{m,\ ATP}$ determination (with YYY peptide fixed at 1mM) for: (**C**) unphosphorylated wild-type (500nM) or mutated (50nM) ALK-TKD; and (**D**) phosphorylated ALK-TKD variants (all at 10nM). (**E**) Comparison of catalytic efficiencies ($k_{cat}/K_{m,\ peptide}$) for unphosphorylated and phosphorylated ALK-TKD variants. (**F**) Comparison of $K_{m,\ ATP}$ values. (**G,H**) Inhibition of unphosphorylated F1174L and R1275Q ALK-TKD (50nM) by crizotinib in peptide phosphorylation assays ([peptide] is 0.5mM) at 0.2mM ATP (**G**) and 2mM ATP (**H**). All

data are shown as means ± SEM from at least three independent experiments. Experiments were performed at 25°C.

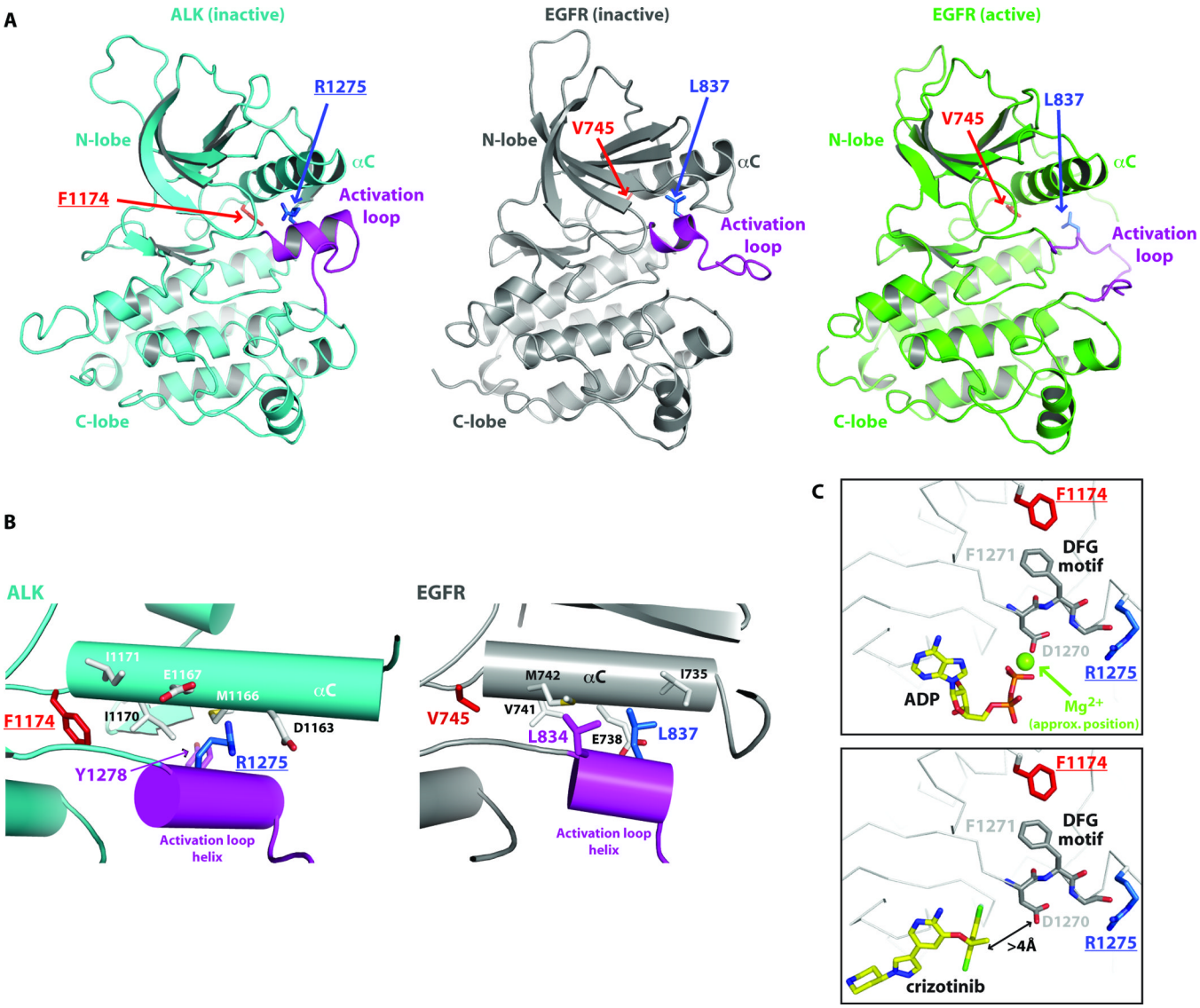

Fig. 6. Structural basis for ALK-TKD activation by F1174L and R1275Q mutations

(**A**) Cartoon representations of inactive ALK-TKD (26) from PDB entry 3LCS (cyan), inactive EGFR-TKD (23) from PDB entry 2GS7 (grey), and active EGFR from PDB entry 1M14 (green). The activation loop is colored magenta in each structure. Positions of F1174 (red) and R1275 (blue) are marked in ALK-TKD, as are their structural equivalents in EGFR (V745 and L837). (**B**) Detail of interactions between the short activation loop helix (magenta) and helix αC in inactive ALK-TKD (left) and inactive EGFR-TKD (right). (**C**) Close-up of relationship between F1174 side chain, the 'DFG motif' and ATP/drug binding site. In the upper panel, taken from PDB entry 3LCT (26), which contains bound ADP, an Mg^{2+} ion (not reported in this structure) was placed based on its location in the active insulin receptor TKD. Lower panel (with bound crizotinib) taken from PDB entry 2XP2.

Table 1

Kinetic parameters of ALK-TKD. Data are shown as mean ± SEM of at least 3 independent experiments. Details of analysis are described in Supplementary Methods. *p* values quoted in the text were determined using an unpaired t-test.

kinase	k_{cat} (min^{-1})	$K_{m,\ peptide}$ (mM)	$k_{cat}/K_{m,\ peptide}$ ($min^{-1} \cdot mM^{-1}$)	$K_{m,\ ATP}$* (mM)	$k_{cat}/K_{m,\ ATP}$ ($min^{-1} \cdot mM^{-1}$)
Wild-type	9.32 ± 0.85	2.88 ± 0.42	3.41 ± 0.44	0.134 ± 0.007	69.7
R1275Q	119 ± 13	2.56 ± 0.32	46.8 ± 1.9	0.326 ± 0.033	364
F1174L	365 ± 61	9.18 ± 1.43	39.7 ± 2.8	0.127 ± 0.011	2870
pWild-type	424 ± 63	1.80 ± 0.17	237 ± 35	0.159 ± 0.012	2660
pR1275Q	347 ± 15	1.39 ± 0.10	252 ± 24	0.248 ± 0.015	1400
pF1174L	436 ± 51	1.25 ± 0.20	357 ± 25	0.109 ± 0.001	3980

*Determined at 1mM peptide.